Nonlinearity and Noise Effects in Multi-level Signal Millimeter-Wave over Fiber Transmission using Single and Dual Wavelength Modulation

Jeanne James, Pengbo Shen, Anthony Nkansah, Xing Liang and Nathan J. Gomes, *Senior Member, IEEE*

Abstract— **We transmit multilevel Quadrature Amplitude Modulation (QAM) data — IEEE 802.16 schemes—at 20MSps and an Orthogonal Frequency-Division Multiplexing (OFDM) 802.11g signal (54Mbps) with a 25GHz millimeter-wave over fiber system, which employs a dual wavelength source, over 20 km of single mode fiber. Downlink data transmission is successfully demonstrated over both optical and wireless (up to 12m) paths with good error vector magnitude. An analysis of two different schemes, in which data is applied to one (single) and both (dual) of the wavelengths of a dual wavelength source, is carried out. The system performance is analyzed through simulation and a good match with experimental results is obtained. The analysis investigates the impact of Mach-Zehnder modulator (MZM) and RF amplifier nonlinearity and various noise sources, such as laser relative intensity noise, amplified spontaneous emission, thermal, and shot noise. A comparison of single carrier QAM IEEE 802.16 and OFDM in terms of their sensitivity to the distortions from MZM and RF amplifier nonlinearity is also presented.**

***Index Terms*— Millimeter-wave over fiber system, DWDM thin film filter, optical phase modulator.**

I. Introduction

The exponential development of mobile communications and the congestion in spectrum allocation, has led to the expectation that wireless systems will move to higher frequencies, and thus the ongoing exploration into millimeter-wave over fiber systems. A number of experimental demonstrations of millimeter-wave over fiber systems using recent standards such as worldwide interoperability for microwave access (WiMAX) IEEE 802.16 [1] and IEEE 802.15.3c (pre-standard millimeter-wave based wireless personal area network – WPAN) [2] have been performed by different research groups. This shift of wireless systems towards millimeter-wave frequencies leads to smaller cell sizes (pico cells), requiring a large number of remote antenna units (RAU) to be deployed for a given coverage area. Then millimeter-wave over fiber systems offer the benefits of high system capacity and low loss of optical fibers, with the requirement of compact and low-cost RAUs, possible if the signal processing functions can be concentrated at a central unit (CU) [3].

To date a number of schemes have been proposed and experimentally demonstrated by different research groups [4]-[8]. Among them, the dual wavelength scheme is promising as it provides a simple system, offers good flexibility in the carrier frequency generation, independent of the data modulation, and does not need a high speed data modulator [8]. The dual wavelength source can be set-up as a mode-locked laser [9] or by externally modulating the laser [8]. The appropriate sidebands, or wavelengths, for the millimeter-wave generation can be selected by bias tuning, with [8] or without optical filtering [1].

Transmission of high multi-Gb/s data rates through millimeter-wave over fiber links has been a topic of interest for many researchers [10]-[14]. However in these reported experiments, the spectrum efficiency (b/s/Hz) is typically low as simple modulation schemes, such as ASK have commonly been used. The carrier frequency is shifted to the millimeter-wave band since more bandwidth is available; however, in the future it is likely that even millimeter-wave spectrum will need to be used efficiently. All the aforementioned systems incorporated a wireless path in their experiments. However, the wireless coverage was only for point to point links over a specific distance.

We have previously reported the use of an optical phase modulator in conjunction with thin film dense wavelength division multiplexing (DWDM) de-multiplexing filter to generate the dual wavelength source. The significance of this filtering technique is that it offers the possibility of generating a continuum of frequencies [8]. We have illustrated the millimeter-wave over fiber downlink performance by transmitting multilevel modulated signals at 60GHz up to 36Mbps [15] and at 25GHz up to 240Mbps for single carrier modulation and 54 Mbps for orthogonal frequency-division multiplexing (OFDM) – using an emulated wireless local area

Manuscript received January 6, 2010; revised June 29, 2010. This work was carried out as part of the COMCORD project funded by the UK Engineering and Physical Sciences Research Council (EPSRC). J James is in receipt of a studentship from the EPSRC.

The authors are all with the Broadband and Wireless Communications Group, Department of Electronics, University of Kent, Canterbury, CT2 7NT, UK (phone: +44 1227 823719; fax: + 44 1227 456084; email (jesj4@kent.ac.uk).

network (WLAN) IEEE 802.11g signal [16]. The IF data signal is applied to the dual wavelength source by means of a Mach-Zehnder modulator (MZM), as in many other radio over fiber systems, e.g. [17]. We also did a stability test on our system over a measurement period of four hours during which time the system was stable [16].

The work presented here focuses on lower bit-rates (up to 120 Mbps) than others have recently achieved [10]-[14], but higher b/s/Hz efficiency – thus different millimeter-wave channels can be used for different systems. Additionally, an OFDM signal was applied to the millimeter-wave over fiber system, as this can allow for dynamic capacity allocation through orthogonal frequency-division multiple access (OFDMA). In this paper, we aim to transmit from the RAU and receive at the mobile unit (MU) different multilevel modulation signals following the IEEE 802.16 (WiMAX) standard [18], and WLAN 802.11g [19] using error vector magnitude (EVM) as the measure of performance. Note that for operational frequencies from 10–66 GHz in the 802.16-2009 standards [18], the WirelessMAN-SC PHY is based on single-carrier modulation. An analysis of two different transportation methods using dual wavelength source have been carried out. One of the transportation methods is the dual wavelength modulation in which both the wavelengths are modulated. The second transportation method is the single wavelength modulation in which only one of the wavelengths is modulated and then recombined with the un-modulated wavelength. It is the first time we present results for the single wavelength modulation system. Slightly different transportation schemes have been presented by other researchers in [20], [21], where a single wavelength is launched in to the MZM and modulated by an IF signal. Optical filters were used to select the carrier and one of the sidebands. Works have been carried out by other researchers, in terms of analyzing the radio over fiber [22], [23] / millimeter-wave over fiber [24], system performance against noise [22], and nonlinearity [22]-[24]. The analysis is done for both back-to-back systems (no fiber, or fiber patchcords only) [24] and over different lengths of single mode fiber (SMF) [22], [23]. All systems used EVM/BER as a measure of system performance, except [23] which used adjacent channel power ratio (ACPR). In [22], the major noise source was the laser as no optical amplifier was used. Here, we demonstrate a millimeter-wave over fiber system by means of experiments and analyze the limitations of its performance. An analysis using simulations is used to investigate the impact of MZM and RF amplifier nonlinearity and various noises - i.e relative intensity noise (RIN), erbium doped fiber amplifier (EDFA) amplified spontaneous emission (ASE), thermal, and shot noise - on the system performance. The non-linear transfer functions of the MZM and RF amplifier cause distortion to the data signals thus degrading the signal quality. Finally, we present results for realistic system operation – over whole coverage areas and not just for point-to-point links over a specific distance. The experimental setup of the proposed system is described in more detail in Section II, whilst measurement results are reported in Section III which also shows a comparison of the experimental, measured results with the simulation results (from VPI TransmissionMaker™) for the proposed millimeter-wave over fiber downlink system. This is followed by Conclusions in Section IV.

II. EXPERIMENTAL SETUP

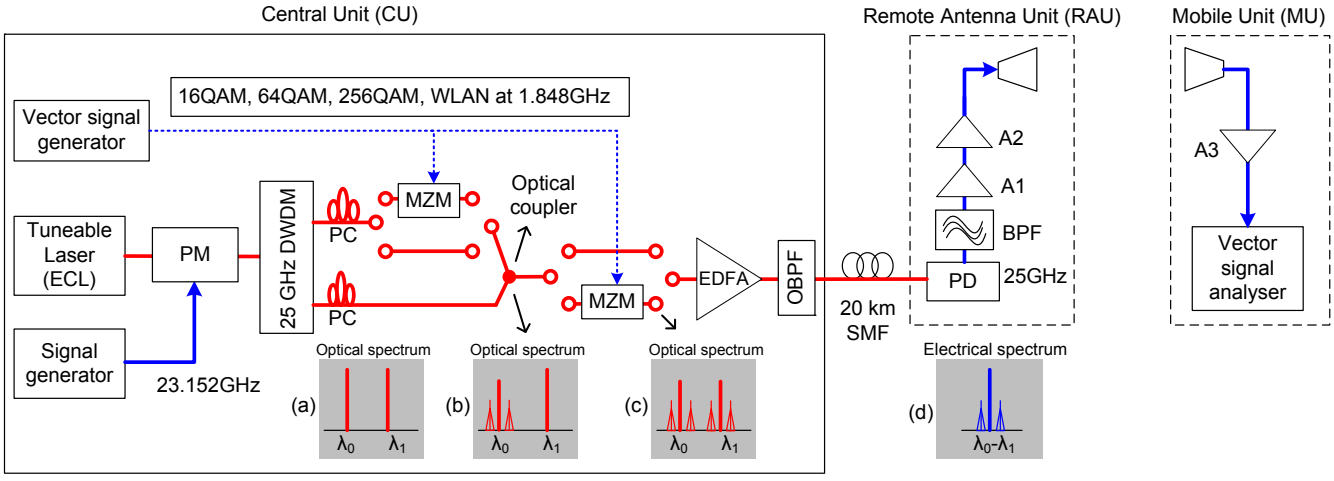

Fig. 1. Downlink experimental setup. ECL: External Cavity Laser, PM: Phase Modulator, PC: Polarization Controller, MZM: Mach Zehnder Modulator, EDFA: Erbium doped Fiber Amplifier, OBPF: Optical band pass filter, PD: Photodiode, A1 – A3: RF Amplifiers.

The downlink experimental setup for optical millimeter-wave generation using the coherent dual wavelength source and data modulation of single wavelength or dual wavelengths is shown in Fig. 1. A Vector Signal Generator (VSG) was used to emulate the IEEE 802.16 modulation schemes [18], and WLAN 802.11g at 54 Mbps [19] at an intermediate frequency (IF) of 1.848 GHz. The modulation schemes specified in the IEEE 802.16 standard [18] consist of quadrature phase-shift keying (QPSK), 16QAM, and 64QAM schemes. A Nyquist square-root raised cosine pulse-shaping filter with a roll-off factor of 0.25 was used.

A continuous wave lightwave of power +5 dBm, was generated by a tunable laser, an external cavity laser (ECL) at

optical angular frequency ω_o. The optical millimeter-wave was generated using an optical phase modulator (PM) along with a DWDM de-multiplexing filter. The PM was driven by a 23.152 GHz RF signal (angular frequency, ω_{RF}). The optical power in the desired optical sidebands is maximized by adjusting the power level of the RF drive signal to the PM. The phase modulated signal can be expressed as:-

$$E_p = E_o \sum_{n=-\infty}^{\infty} J_n(\beta_p)\, e^{j(\omega_o + n\omega_{RF})t} \quad (1)$$

where E_o is the amplitude of the light source, β_p is the modulation index of the phase modulator and J_n is the Bessel function of the first kind of order n. In our case, the power in each of the first-order sidebands is made equal to that in the carrier. The carrier and the upper first-order sideband are selected by a 25 GHz spacing DWDM de-multiplexing filter and polarization aligned by polarization controllers to generate a coherent dual wavelength source, as shown in Fig. 1 as inset (a). The port-to-port insertion loss of the DWDM de-multiplexing filter per channel is approximately 6dB.

The mathematical expression for the optical signal after the DWDM de-multiplexing filter which is shown as inset (a) in Fig. 1 can be expressed as

$$E_f = \beta_k\, E_o\{cos(\omega_o + \omega_{RF})t + cos\omega_o t\} \quad (2)$$

where $\beta_k$is the modulation index of the phase modulator when the power on the first order sidebands is made equal to that in the carrier.

The optical signal for the single wavelength modulation at the input of the EDFA shown as inset (b) in Fig. 1 can be expressed as

$$E_s = \beta_k E_o\{cos(\omega_0 + \omega_{RF})\, t + (1/\sqrt{2})[cos\omega_0 t - (\beta_i/2)[cos[\omega_0 - \omega_{IF}]\, t + cos[\omega_0 + \omega_{IF}]\, t]]\} \quad (3)$$

where β_i is the modulation index of the MZM and ω_{IF} is the angular frequency of the IF data signal applied to the MZM.

The optical signal for the dual wavelength modulation at the input of the EDFA shown as inset (c) in Fig. 1 can be expressed as

$$E_d = (E_o\, \beta_k/\sqrt{2})\{[cos\omega_0 t - (\beta_i/2)[cos(\omega_0 - \omega_{IF})\, t + cos(\omega_0 + \omega_{IF})\, t]] + [cos\,(\omega_0 + \omega_{RF})t - (\beta_i/2)[cos[(\omega_0 + \omega_{RF}) - \omega_{IF}]\, t + cos[(\omega_0 + \omega_{RF}) + \omega_{IF}]\, t]]\} \quad (4)$$

The data modulation was applied either to one (single) or to both (dual) wavelengths. For single wavelength modulation, the data modulated carrier and the un-modulated upper first order sideband are coupled together using a 3dB optical coupler. For dual wavelength modulation, both the carrier and the upper first order sideband are data modulated after the 3dB optical coupler. The optical spectra arising from single and dual wavelength modulation are shown in Fig. 1 as inset (b) and (c) respectively. Different millimeter-wave frequencies can easily be generated using this filtering technique [8].

The IF data signals (QPSK, 16QAM, 64QAM, 256QAM and WLAN 802.11g) were applied to the MZM biased at its quadrature point – the fundamental detected RF signal at the photodiode receiver was maximised. The V_π of MZM was 5V. The input optical power to the EDFA measured on a power meter was around -13.5 dBm and -20.5 dBm for single and dual wavelength respectively. The ECL optical power was +5dBm and this shows that the optical loss of the millimeter-wave generation technique with the MZM insertion loss (7dB) was 18.5 dB and 25.5 dB for single and dual wavelength respectively. This is the typical loss in milllimeter-wave generation techniques using sideband filtering [25]. The modulated optical sidebands are amplified by an EDFA and filtered by an optical DWDM filter of 50 GHz channel spacing to reduce the Amplified Spontaneous Emission (ASE) noise.

The filtered signal is fed into a SMF of 20 km length and terminated by a 65GHz photodiode (PD) with a responsivity of 0.5A/W, where the optical signal is converted back to RF. The generated photocurrent (I_s).of the single wavelength modulation can be written as

$$I_s = R * (E_s * \overline{E_s}) \quad (5)$$

where R is the (frequency dependent) responsivity of the photodiode and E_s is the output optical signal of the single wavelength modulation. This assumes that the EDFA compensates for filtering and fiber transmission loss, and neglect noise, for simplicity. There will be a similar formulation for generated photocurrent (I_d) of the dual wavelength modulation.

The detected photocurrent I_s for single wavelength modulation at inset (d) in Fig. 1 can be expanded as

$$I_s = R * [\beta_k E_o]^2 * \{3/2 + \beta_i{}^2/4 - \beta_i cos\omega_{IF} t + (\beta_i{}^2/4)cos2\omega_{IF} + \sqrt{2}\, cos\omega_{RF} t - (\beta_i/\sqrt{2})[cos(\omega_{RF} + \omega_{IF})t + cos(\omega_{RF} - \omega_{IF})]t\} \quad (6)$$

The detected photocurrent I_d for dual wavelength modulation at inset (d) in Fig. 1can be expanded as

$$I_d = R * [E_{cw}\, \beta_k/\sqrt{2}]^2 * \{2 + \beta_i{}^2 - 4\beta_i cos\omega_{IF} t + \beta_i{}^2 cos2\omega_{IF} t + (2 + \beta_i{}^2) * cos\omega_{RF} t - 2\beta_i[cos(\omega_{RF} + \omega_{IF})t + cos(\omega_{RF} - \omega_{IF})t] + (\beta_i{}^2/2)[cos(\omega_{RF} + 2\omega_{IF})t + cos(\omega_{RF} - 2\omega_{IF})t]\} \quad (7)$$

In this paper the term involving $cos(\omega_{RF} + \omega_{IF})t$ generates the 25GHz data signal which is selected using an electrical band pass filter. The RAU consists of a PD, band-pass filter (BPF), low-noise amplifier (A1), and power amplifier (A2) and a directional horn antenna of gain 20dBi, which emits the millimeter-wave signal wirelessly to the MU as depicted in Fig. 1. Quite high antenna gain is also achievable with other configurations (omni-directional antenna in the horizontal plane), which are suitable for providing full coverage, as some of our other work has shown [26]. The MU has a directional horn antenna of gain 20dBi, a low-noise amplifier (A3) and an Agilent Vector Signal Analyzer (VSA). The VSA consists of an Agilent PSA series spectrum analyzer connected to a laptop with Agilent VSA software for EVM measurements. The VSA has the capability of measuring signals with frequencies up to 26.5GHz.

III. MEASUREMENT RESULTS

A. *Phase noise of generated millimeter-wave signal*

The phase noise of the generated millimeter-wave signal can degrade data modulated signals. For this reason it is important that the beating of the optical sidebands of the phase modulated signal (dual wavelength source) produces a high quality millimeter-wave signal [8], [27]. A phase noise of -105.54dBc/Hz at 100kHz offset from the carrier (23.152 GHz) was measured when no data modulation was applied to the MZM and the performance did not degrade after transmission through 20 km length of SMF. There may be slower phase drift as a result of the fiber transmission, but this is corrected in typical multi-level signal demodulation schemes.

B. *EVM requirements*

The minimum EVM requirements in the frequency range of 10-66GHz, for an IEEE 802.16-2009 standard [18] base-station transmitter is shown in Table I. There are three symbol rates (16, 20, and 22.4MSps) specified in the IEEE 802.16 standard. The performance of the proposed system was studied for a symbol rate 20MSps. However, the proposed system configuration can support higher symbol rates [16] and multiple users by simultaneously transmitting many such channels [28], as we have demonstrated previously.

TABLE I

EVM REQUIREMENTS FOR (IEEE 802.16) WIMAX TRANSMITTER

Modulation scheme	rms EVM (%)/SNR (dB) required	
	without equalization	with equalization
QPSK	12/18.4	10/20
16QAM	6 / 22	3 / 28
64QAM	3.1 / 26.5	1.5 / 33

TABLE II

EVM REQUIREMENTS FOR (IEEE 802.16) WIMAX RECEIVER

Modulation scheme	rms EVM (%)/SNR (dB) required
QPSK	32.4 / 9.8
16QAM	10.8 / 16.8
64QAM	4.7 / 23

C. *Experimental results of downlink performance for dual and single wavelength data modulation*

The quality of the generated data modulated millimeter-wave signal was checked using root mean square (rms) EVM measurements for different input power levels. Note an equalizer was used to remove the effect of the source channel impairment to improve the signal quality of the source. The rms EVM (over 1000 symbols) and signal power averaged over five sets of 100 such measurements for the proposed system was recorded at the VSA, using a macro program. Thus, the mean rms EVM was calculated from all 500 rms EVM readings. Note a symbol rate of 20MSps was used instead of higher symbol rates (30MSps) possible in the experiment because of limitations with the simulations. For higher symbol rates, the simulation required a longer time window to gain enough data points, which could not be achieved due to insufficient computation resources.

In single wavelength modulation, only one of the wavelengths experiences MZM insertion loss (7dB) in contrast to the dual wavelength modulation. Hence the total optical power at the input of the EDFA is 7dB higher in the single compared to the dual wavelength modulation technique. In order to prevent damage to the PD the output optical power of the EDFA was attenuated by 1dB in single wavelength modulation. In dual wavelength modulation, no optical attenuators were used before the PD.

Fig. 2.a and 2.b shows the average rms EVM of single carrier QAM at a symbol rate of 20MSps, for different input IF drive power levels to the MZM for dual wavelength modulation. Two different configurations: back-to-back (Fig.2.a) and after a 20 km length of SMF (Fig. 2.b) are shown. The power shown in Fig. 2.a and 2.b is the power level of the modulated millimeter-wave signal (64QAM) at the input of the transmitter antenna. The measured average rms EVM of the WLAN 802.11g (54Mbps) OFDM signal is also shown in Fig. 2.a and 2.b.

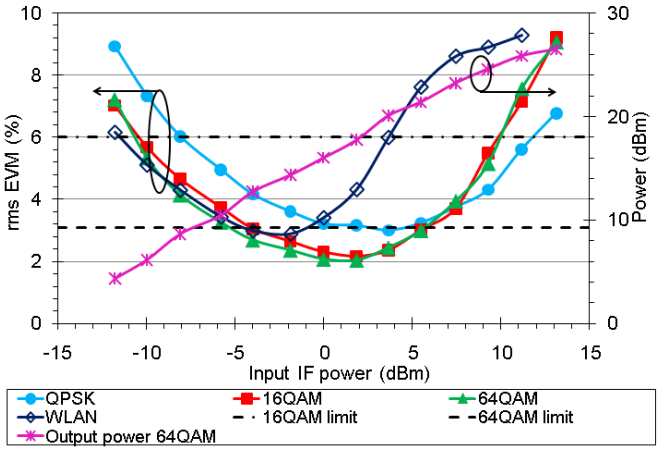

(a)

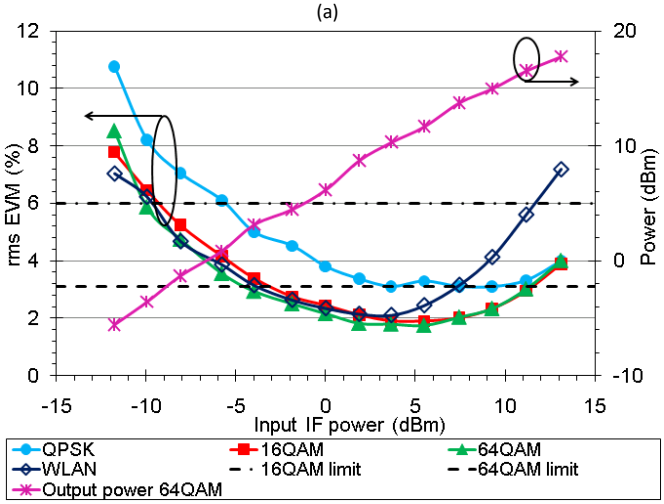

(b)

Fig. 2. Average rms EVM and power at symbol rate 20MSps for dual wavelength modulation in (a) back-to-back configuration and (b) after 20 km SMF.

The lines between symbols are only an aid for viewing the results and do not represent predicted trends.

Fig. 3.a and 3.b shows the average rms EVM of single carrier QAM at a symbol rate of 20MSps, for different input IF drive power levels to the MZM, for singe wavelength modulation. EVM results are for the two different configurations: back-to-back (Fig. 3.a) and after a 20 km length of SMF (Fig. 3.b). The power shown in Fig. 3.a and 3.b is the power level of the modulated millimeter-wave signal (64QAM) at the input of the transmitter antenna.

For comparison, the 802.16 transmitter EVM limits for 16 and 64QAM levels are also shown in Fig. 2 and Fig. 3. QPSK was within the EVM limit of 12% for all power levels shown (measured) and for both configurations in Fig.2.a and Fig. 2.b. Further experiments were carried out with a slight modification of the emulated 802.16 specifications by increasing the QAM level to 256. As the 802.16 standard does not include 256QAM, the Digital Video Broadcasting standard's 256QAM EVM requirement of 2% was used [29]. The EVM limit for 256QAM is shown in Fig. 3. Experiments were done with 256QAM for single wavelength modulation only as it was clear that this system had better performance than the dual wavelength modulation. Multilevel modulation schemes (16, 64 and 256QAM) and OFDM (WLAN 802.11g) are sensitive to nonlinear distortions. In practice, when the power of the driving signal to the MZM increases, the nonlinear transfer function of the MZM distorts the signal and degrades the EVM for both single carrier QAM (16, 64 and 256QAM) and OFDM. However the MZM nonlinearity has much stronger impact on OFDM than on single carrier QAM, due to the multiple subcarriers causing higher peak-to-average power levels and generating more inter-modulation products. In the back-to-back configuration, the EVM degrades more quickly at the higher IF power region compared to the EVM results after transmission through the 20 km SMF. Thus with the inclusion of the 20 km SMF, the nonlinearity of the system is shifted to the much higher input power region. This input power shift will be explained in sub-section D.

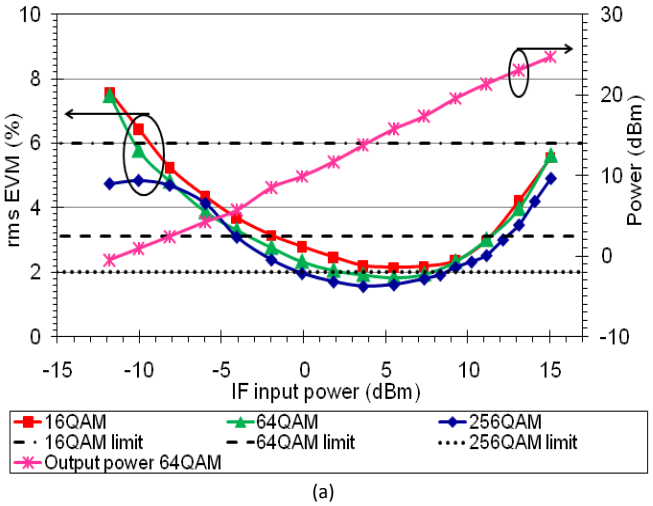

(a)

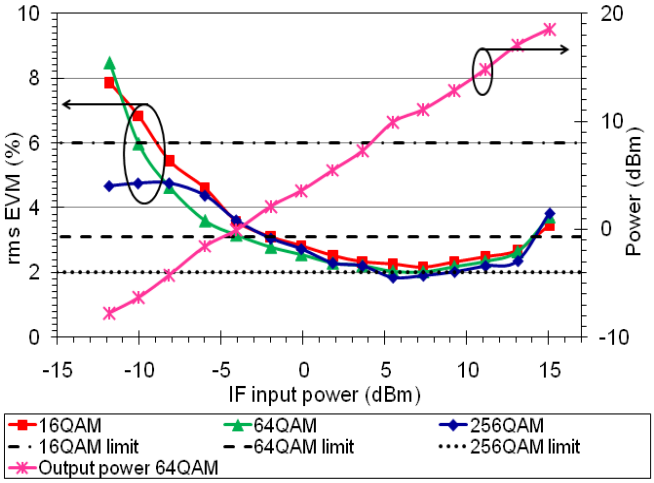

(b)

Fig. 3 Measured average rms EVM and power at symbol rate 20MSps for single wavelength modulation in (a) back-to-back configuration and (b) after 20 km SMF.
Note: A 1dB optical attenuator was included at the PD input in single wavelength modulation.

D. Simulation results of downlink performance for dual and single wavelength data modulation

The downlink millimeter-wave over fiber system in the experimental set up was simulated in Virtual Photonics Inc. (VPI) software. A QAM transmitter model was used to generate different multilevel QAM signals and a QAM receiver model was used at the receiver for EVM analysis. The relative intensity noise (RIN) of the ECL and the noise figure of EDFA was measured to be of -150dB/Hz and 5dB respectively. These measured values are used in the simulation. The Agilent VSA has an input noise of -132.2dBm/Hz (41.8dB noise figure) at 25GHz. Hence, the 41.8dB noise figure is included as an additional input noise at the QAM receiver model using an electrical amplifier model with its gain and current noise spectral density set to 0dB and 1.10062nA/√Hz (equivalent to the 41.8dB noise figure) respectively. The simulation analysis conducted here, investigates the impact of MZM and RF amplifier nonlinearity and various noises (i.e RIN, thermal, EDFA ASE, and shot noise) on the downlink millimeter-wave over fiber system.

In order to focus only on the MZM nonlinearity, no RF amplifiers are included at this stage in the simulation and the noise in all of the components (i.e. RIN, ASE noise, shot and thermal noise,) was deactivated. The MZM was driven at an IF power of -10 to 14 dBm. Fig. 4 shows the simulated EVM results for single carrier 64QAM at 20MSps for dual wavelength modulation. When all the noises are deactivated, poor EVM is observed at the higher IF power region due to the MZM nonlinearity. To investigate the noise in the lower IF power region where noise dominates performance, a single noise source was activated at a time. As illustrated in Fig. 4, the main noise contribution results from the EDFA ASE noise; without the optical amplifier, RIN is dominant. The EVM curves shown in Fig. 4 are for the dual wavelength data modulation technique.

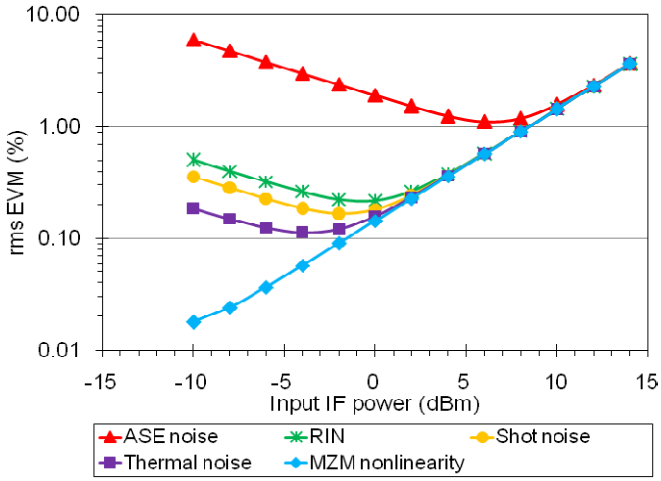

Fig. 4. Simulated EVM versus IF drive power to the MZM with laser RIN, ASE, shot and thermal noise parameters for single carrier 64QAM at 20MSps

Noise was activated in all of the components and a comparison of degradation of EVM by the MZM nonlinearity for different modulation schemes (QPSK, 16QAM and 64QAM), at a symbol rate of 20MSps in back-to-back configuration is shown in Fig. 5. It is seen that at the higher IF power region, QPSK can handle an additional 4dB of input power compared to 64QAM for the same signal-to-noise ratio (SNR). This demonstrates the sensitivity of the higher level modulation schemes (16QAM and 64QAM) to nonlinear distortions by the MZM. However at the lower IF power region, the SNR is similar for all the modulation schemes since this region is dominated by noise (as illustrated in Fig. 4). As the symbol rate is constant (constant bandwidth), the noise power is fixed for all the modulation schemes resulting in similar SNR. Note that at the higher IF power region where the non-linearity of the MZM increases the EVM, the SNR then becomes signal to noise plus interference ratio. The interference aspect is due to the unwanted third order distortion of the MZM interfering with the signal.

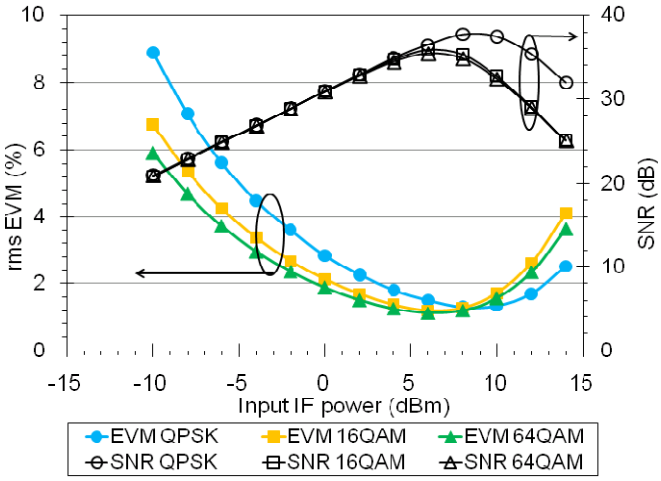

Fig. 5. Simulated EVM and SNR results versus different modulation schemes and for a symbol rate of 20MSps

The nonlinearity of the RF amplifiers is a very important characteristic that limits the capabilities of the millimeter-wave over fiber system. While RF amplifiers may be essential for the reception of faint signals, strong signals will lead to distortion in the amplifier and/or subsequent components. This dynamic range in the signals is significant in wireless systems, and therefore for radio over fiber systems which have to deal with variable distances between mobile/wireless users. Downlink dynamic range is important to keep the RAU as simple as possible (without power control) and for broadcast/multicast transmissions, as the mobile receivers may be at different distances from the RAU.

Simple polynomial expressions are used to characterize the nonlinear transfer function of the RF amplifiers used in the experimental millimeter-wave over system, in order to predict their impact on the EVM performance. The polynomial expression (AM/AM model) was derived from curve fitting of measured data at 25GHz. The polynomial expressions for the RF amplifiers A1, A2 and A3 are given in (8) (9) and (10), respectively. The noise figures of 2.8dB (8.51311pA/√Hz) and 7dB (17.9195pA/√Hz) were used for the RF amplifiers A1 and A2, respectively. The coefficients of the polynomial expressions are determined based upon the measured power levels that the resultant-order term would produce. The polynomial expressions and the coefficients of these RF amplifiers are given in Table III.

$$y = a_0 + a_1x + a_2x^2 + a_3x^3 + a_4x^4 + a_5x^5 + a_6x^6 \quad (8)$$

$$y = b_0 + b_1x + b_2x^2 + b_3x^3 + b_4x^4 + b_5x^5 + b_6x^6 + b_7x^7 + b_8x^8 \quad (9)$$

$$y = c_0 + c_1x + c_2x^2 + c_3x^3 + c_4x^4 + c_5x^5 + c_6x^6 \quad (10)$$

where x represents the input amplitude.

TABLE III

THE COEFFICIENTS FOR AM/AM MODEL

Coefficients for AM/AM model for measurements at 25GHz					
a_0	-0.0048	b_0	-0.03779	c_0	0.0223
a_1	47.041	b_1	24.93	c_1	22.187
a_2	-555.42	b_2	-256.5	c_2	118.21
a_3	2262	b_3	2242	c_3	-3076.1
a_4	6944.9	b_4	-8536	c_4	19125
a_5	-81095	b_5	1.659e04	c_5	-51148
a_6	173398	b_6	-1.749e04	c_6	51040
		b_7	9546		
		b_8	-2121		
		b_8	-2121		

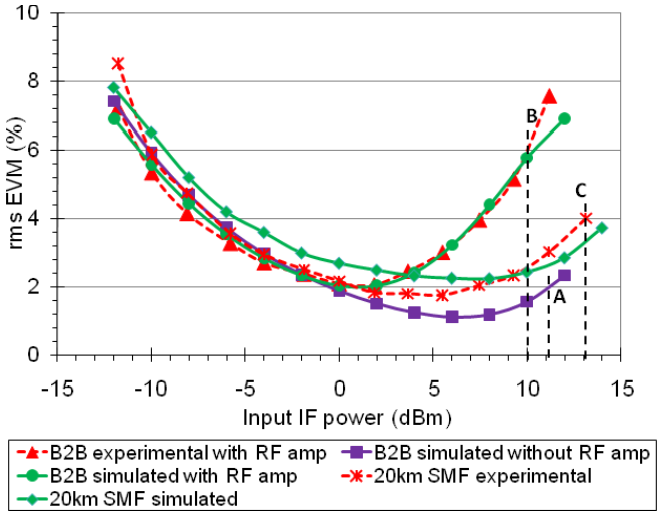

(a)

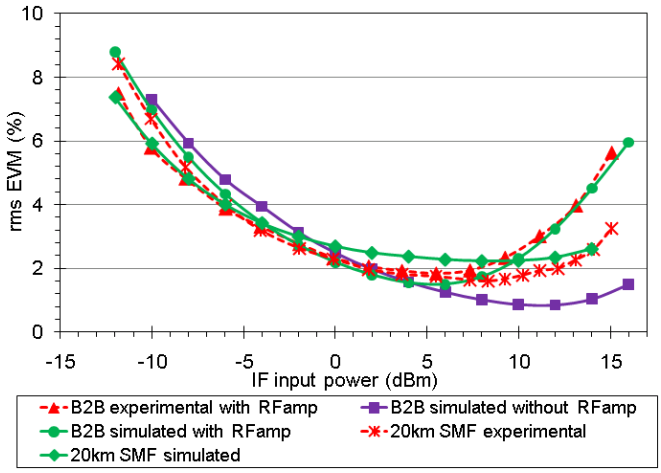

(b)

Fig. 6 Simulated and measured EVM results for single carrier 64QAM at 20MSps in back-to-back (B2B) and after 20 km SMF configuration for (a) for dual wavelength modulation and (b).for single wavelength modulation.
Note: 1dB optical attenuator was included at the PD input in single wavelength modulation.

Fig. 6.a and 6.b shows the simulated and measured EVM results for different IF drive powers to the MZM for dual and single wavelength modulation, respectively. The EVM curves are for single carrier 64QAM at 20MSps in back-to-back and 20km SMF configuration. Note that the VSA noise figure (NF) was not included when obtaining the EVM curves without RF amplifiers in back-to-back configuration (Fig. 6). It can be observed that in the back-to-back configuration in the absence of RF amplifiers, the MZM nonlinearity dominates at the higher IF power region, causing an increase in the EVM (Fig. 6.a and 6.b). With the inclusion of the RF amplifier, when the signal level is within the linearity limits of the RF amplifier (at the lower IF power region), the EVM is similar to the EVM results without the RF amplifiers. However as the IF drive power increases the RF amplifier nonlinearity rapidly degrades the system, thereby increasing the EVM value. Due to large path loss at millimeter-wave frequencies [32], RF amplifiers are required to provide sufficient power at the RAU, and this will be explained further in subsection F. Note that the transmitted EVM must be within the specific wireless standards under test transmitter EVM requirements.

In the simulation, for the SMF model, a chromatic dispersion (CD) of 16 ps/nm/km and attenuation (α) of 0.2dB/km was considered. Note that the EVM curves in Fig. 6.a and 6.b for the 20km SMF configuration includes the RF amplifiers (A1 and A2). For an IF power of -12dBm to the MZM, for dual wavelength modulation, the EVM increased from 6.8% for the back-to-back configuration to 8.2% for 20km fiber propagation (Fig. 6.a). For single wavelength modulation, the EVM increased from 7.4% to 8.4%. The EVM increase is due to an RF power loss of 9dB after propagating through the 20km SMF. In dual wavelength modulation (Fig. 6.a), for an IF power of 10dBm to the MZM, the EVM improved from 5.6% to 2.8% in the 20km SMF configuration compared to the back-to-back. For the same RF power of 10dBm in single wavelength modulation (Fig. 6.b), the EVM improved from 2.6% (back-to-back) to 1.8% (20km SMF). Unlike the back-to-back configuration, the RF signal power is now well within the linearity limits of the RF amplifier (A2) in the 20km SMF configuration causing an improvement in the EVM. The MZM input 1dB compression point (P1dB) at 25GHz was measured as 12dBm. Thus, the MZM nonlinearity is the limiting factor with the inclusion of 20 km SMF.

In VPI, an OFDM transmitter model was used to emulate the 802.11g signal and an OFDM receiver model was used at the receiver for EVM analysis. In the simulation, a 64QAM OFDM with a symbol rate of 10MSps (data rate 60 Mbps) was used instead of 9MSps (data rate 54 Mbps) because VPI requires the number of symbols (ratio between the time widow and symbol rate) to be a power of two. A Nyquist square-root raised cosine pulse-shaping filter with a roll-off factor of 0.5 was used. The length of the cyclic prefix was set to 1/8.

Fig. 7 shows the simulated and measured EVM results for OFDM (WLAN 802.11g) in back-to-back and after 20km SMF configuration for dual wavelength modulation. It can be noticed that when the IF drive power was larger than 0dBm, the dramatic increase in EVM shows a larger degradation of the system performance for the OFDM signal (Fig. 7) compared to the single carrier QAM signal (Fig. 6.a). As example points of comparison, in back-to-back configuration for the single carrier QAM (Fig. 6.a) and OFDM (Fig. 7) signals, in the absence of RF amplifiers and with the inclusion of RF amplifiers, points A and B, corresponding to EVM values of 2% and 6% have been indicated in the figures. At these points, the IF drive signal to the MZM for the OFDM was 7dBm and 3.8dBm compared to the single carrier QAM signal power levels of 11dBm and 10dBm without and with RF amplifiers, respectively. This indicates more stringent electrical power budget for OFDM, even though the OFDM signal (WLAN 802.11g, 9MSps) has approximately half the symbol rate compared to the single carrier QAM (20MSps). The RF amplifiers at the transmitter are linear only within a limited dynamic range. Due to the OFDM signal's high peak to average ratio (PAPR) [30], OFDM suffers more from non-linear distortions due to clipping than single carrier QAM. To avoid such distortions, the RF amplifiers have to be operated

with large power back-off, but this leads to inefficient use of the amplifiers. However at the lower IF power region, poor EVM is observed for both OFDM and single carrier QAM signal due to reduced SNR, as this region is dominated by noise (as shown in Fig. 4).

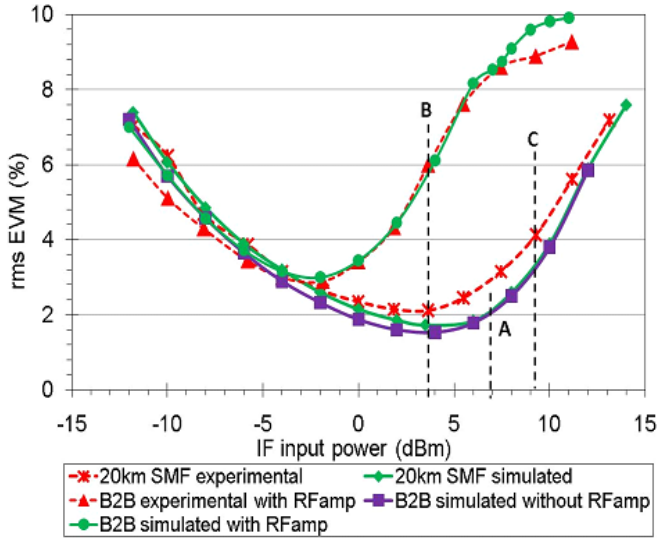

Fig. 7 Simulated and measured EVM results for OFDM (WLAN 802.11g) in back-to-back (B2B) and after 20km SMF configuration for dual wavelength modulation.

Note that the EVM curves in Fig. 7 for the 20km SMF configuration includes the RF amplifiers (A1 and A2). At point C (Fig. 6 and Fig. 7) for the same EVM of 4%, IF drive signal to the MZM for the OFDM was 9.2dBm compared to the single carrier QAM signal power level of 13dBm. This clearly indicates that as with the single carrier QAM case (Fig. 6), the OFDM (WLAN 802.11g) transmission is limited by the MZM nonlinearity with the inclusion of 20 km SMF.

E. Comparison of results for dual wavelength and single wavelength modulation

Fig. 8 shows the comparison of single and dual wavelength modulated EVM results (experimental) for 64QAM at 20MSps in back-to-back and after 20km SMF configurations. The x-axis is the power level of the generated modulated millimeter-wave signal at the output of the RF amplifiers (at the RAU). The nonlinearity limitations for both the signal and dual wavelength modulated EVM results are caused by the RF amplifiers (at the RAU) and the MZM (at the CU) for the back to back and after the 20km fiber respectively. This can be observed in Fig. 8 as the back to back EVM increases at a much higher output power (+19.5dBm) compared to the 20km SMF configuration (+11.5dBm).

The single wavelength modulation has 5dB lower RF gain and thus a 5dB higher input drive power is required at the MZM to obtain the same RF output power as the dual wavelength modulation. Note 1dB optical attenuator was included at the PD input in single wavelength modulation for both back-to-back and after 20km SMF configurations for protection of the PD in the former. The effect of the higher input RF drive power at the MZM of the single wavelength modulation results in lower EVM values at the lower output power region from -9dBm to +8dBm (20km fiber), +1dBm to +16dBm (back to back) than the dual wavelength modulation as shown in Fig. 8.

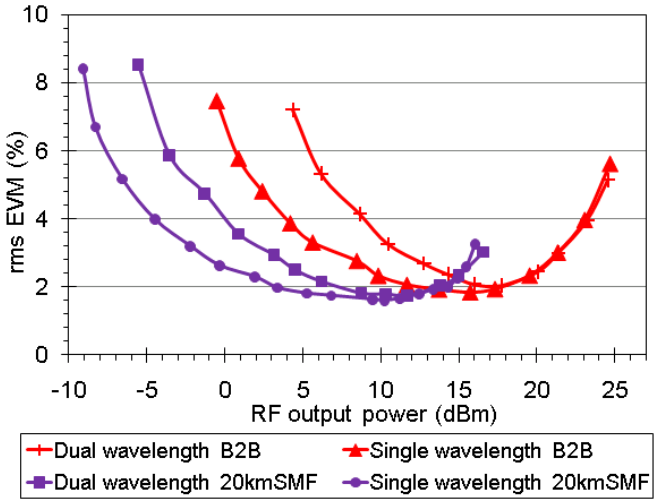

Fig. 8 Measured RF output power (at RAU amplifier) vs. EVM results for 64QAM at 20MSps for single wavelength and dual wavelength modulation in back-to-back (B2B) and after 20km SMF configuration.
Note: A 1dB optical attenuator was included at the PD input in single wavelength modulation.

F. Experimental and simulation results for downlink wireless path

For the wireless measurements, the input power to the MZM was set to 5dBm. The RAU transmit power in EIRP (Effective Isotropic Radiated Power) was 31.2dBm. The frequently used Keenan-Motley path loss L_p model for indoor environments was used in the simulation [31]. Ignoring the effects of transmission loss through walls and floors, the Keenan-Motley equation reduces to the open space path loss equation with a modified path loss exponent n [32].

$$L_p = (4\pi f/c)^2 d^n \quad (11)$$

where f is the frequency of the RF signal (25GHz), c is the velocity of light, and d is the distance between the transmitter (RAU) and the receiver (MU). The path loss exponent n is a characteristic of the propagation environment and a value of 3 was used in the simulation

After propagating through the wireless path, the signal is received by a 20dBi horn antenna and a LNA (A3). The inclusion of the RF amplifier at the MU will enable longer wireless distance transmission. However there will be a need to define a minimum distance between RAU and MUs, to prevent overdriving the MU's RF amplifiers. In order to examine the wireless coverage, EVM measurements were carried out at different points over a 12m range (the maximum wireless range possible in our laboratory), The EVM values (simulated and measured) for single carrier 64QAM at 20MSps and WLAN (OFDM) are plotted in Fig. 9.a and 9.b. Note the wireless measurements were done only for dual wavelength modulation. Distance zero corresponds to the

EVM at the input of the RAU horn antenna (downlink transmitter). There is a sudden increase in EVM when the MU is 1m away from the RAU (Fig. 9.a and 9.b). Separate measurements were carried out to confirm that this sudden increase in EVM is from overdriving the RF amplifier (A3) at the MU, as they were not apparent when the input power was reduced. An EVM of 4.7% and 3.2% at 1m and 12m wireless distance has been achieved for single carrier 64QAM, meeting the IEEE 802.16 receiver EVM requirement (Table II). However for WLAN OFDM (Fig. 9.b), the minimum distance between RAU and MU with an EVM within the standards' requirement is 2m. An EVM of 3.4% and 2.2% at 2m and 12m wireless distance has been achieved for WLAN OFDM meeting the IEEE 802.11g standard [19].

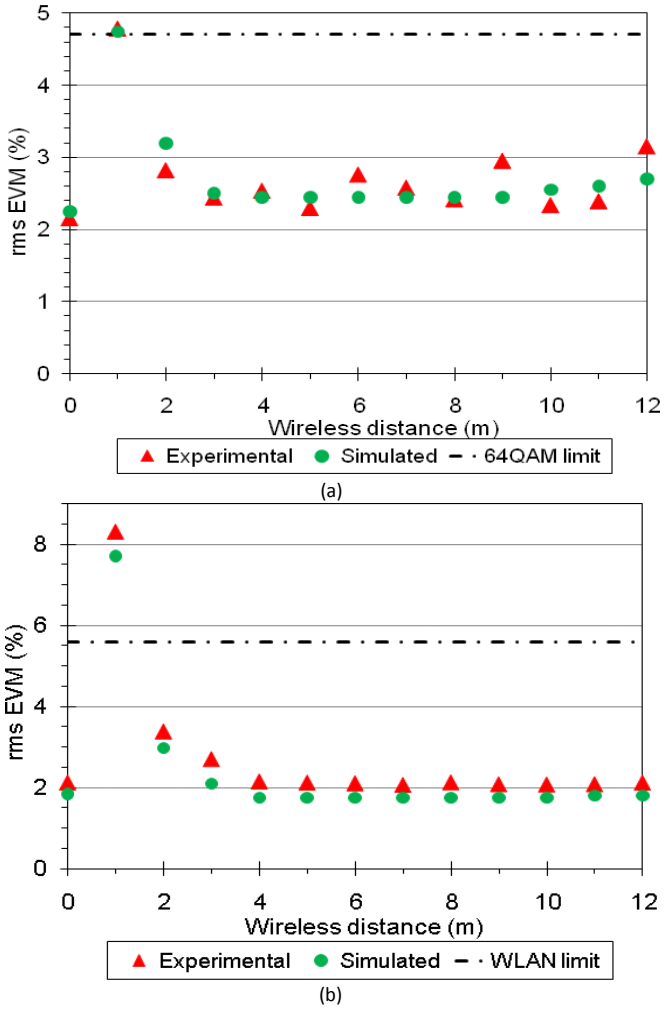

Fig. 9 Simulated and measured EVM for different wireless distances for dual wavelength modulation (a) single carrier 64QAM at 20MSps and (b) OFDM (WLAN 802.11g.
Note: Distance zero is the EVM at the input of the transmitter antenna.

IV. Conclusion

Successful transmission of emulated multilevel modulated WiMAX signals at 20MSps and WLAN 802.11g at 54Mbps over a 25GHz millimeter-wave optical and wireless downlink was demonstrated. Both dual and single wavelength modulation techniques were carried out. The measured EVM values match the wireless standards' requirements.

The system performance was studied through simulation and an experimental investigation and the obtained results are in good agreement. As expected, in the lower input RF power region, noise is the limiting factor, of which EDFA ASE noise is the dominant noise in our system. In the higher input RF power region, either amplifier or MZM nonlinearity may dominate, this being closely linked to the RF amplifier gain requirements for wireless coverage. In our system, for the back-to-back configuration, the RF amplifier nonlinearity is the limiting factor. However, with the inclusion of 20 km SMF the signal is within the linearity limits of the RF amplifier and the MZM nonlinearity becomes the limiting factor.

The presented wireless transmission results for the dual wavelength modulation technique are for realistic system operation – over whole wireless coverage areas and not just for point-to-point links over a specific distance. The wireless distance (12m) was limited by laboratory constraints, but suggests reasonable, picocellular shared office areas can be covered by this type of system. In future work, wireless transmission with the single wavelength modulation scheme will be carried out.

Acknowledgement

The authors wish to acknowledge useful discussions with their colleague L. C. Vieira in the University of Kent, Canterbury, U.K. The authors are also grateful to S. Jakes, T. Rockhill and C. Birch for mechanical workshop support and D. Hook for IT support

References

[1] A. Nkansah, A. Das, N. J. Gomes, and P.Shen, "Multilevel Modulated Signal Transmission Over Serial Single-Mode and Multimode Fiber Links Using Vertical-Cavity Surface-Emitting Lasers for Millimeter-Wave Wireless Communications," *IEEE Trans. Microw. Theory Tech*, vol. 55, no. 6, pp.1219–1228, Aug. 2007.

[2] M. Huchard, M. Weiss, A. Pizzinat, S. Meyer, P. Guignard, and B. Charbonnier, "Ultra-Broadband Wireless Home Network Based on 60-GHz WPAN Cells Interconnected via RoF," *IEEE J. Lightw. Technol*., vol. 26, no. 15, pp. 2364-2372, Aug. 2008.

[3] D.Wake, "Trends and prospects for radio over fibre picocells," in *Int.Microw. Photon. Top. Meeting* , Awaji, Japan, Nov. 2002, pp. 21–24.

[4] A. Das, A. Nkansah, N. J. Gomes, I. J. Garcia, J. C. Batchelor, and D. Wake, "Design of Low-Cost Multimode Fiber-Fed Indoor Wireless Networks," *IEEE Trans. Microw. Theory Tech.,* vol. 54, no. 8, pp. 3426-3432, Aug. 2006.

[5] H. Suzuki, M. Fujiwara, K. Iwatsuki, A. Hirata and T. Nagatsuma, "Photonic millimetre-wave generator using intensity and phase modulators for 10 Gbit/s wireless link," *Electron. Lett*., 2005, vol. 41, no. 6, pp. 355–356, Mar. 2005.

[6] C. Park, C. Lee, and C. Park, "Photonic Frequency Upconversion by SBS-Based Frequency Tripling," *IEEE J. Lightw. Technol.*, vol. 25, no. 7, pp.1711–1718, July. 2007.

[7] C. Lim, A. Nirmalathas, D. Novak and. R. Waterhouse, "Optimisation of baseband modulation scheme for millimetre-wave fibre-radio systems," *Electron. Lett.,* vol. 36, no. 5, pp. 442–443, Mar. 2000.

[8] P. Shen, J. James, N. J. Gomes, P. G. Huggard and B. N. Ellison, "Low Cost, Continuously Tunable, Millimeter-wave Photonic LO Generation using Optical Phase Modulation and DWDM Filters," *IEEE Photon. Technol. Lett*., vol. 20, no. 23, pp. 1986-1988, Dec. 2008

[9] M. Attygalle, C. Lim and A. Nirmalathas, "Single monolithic hybrid mode-locked laser for multiple WDM channels mm-wave radio signal

distribution," in *Int. Topical Mtg. on Microw. Photon.* , Budapest, Hungary, pp 31-34, Sep. 2003.
[10] A. Hirata, H. Takahashi, R. Yamaguchi, T. Kosugi, K. Murata, T. Nagatsuma, N. Kukutsu, and Y. Kado, "Transmission Characteristics of 120-GHz-Band Wireless Link Using Radio-on-Fiber Technologies," *IEEE J. Lightw. Technol.,* vol.26, no.15, pp.2338–2344, Aug. 2008.
[11] Y. Hsueh, Z. Jia, H. Chien, J. Yu, and G. Chang, "A Novel Bidirectional 60-GHz Radio-Over-Fiber Scheme With Multiband Signal Generation Using a Single Intensity Modulator," *IEEE Photon. Technol. Lett*., vol. 21, no. 18, pp. 1338-1340, Sep. 2009.
[12] I. Insua, K. Kojucharow, C. Schaeffer, "MultiGbit/s transmission over a fiber optic mm-wave link," in *IEEE MTT-S Int. Microw. Symp.Dig*, Atlanta, Georgia, pp. 495–498, Jun. 2008.
[13] A. Stöhr, M. Weiß, V. Polo, R. Sambaraju, J. L. Corral, J. Marti, M. Huchard, B.Charbonnier, I. Siaud, S. Fedderwitz, and D. Jäger, "60 GHz radio-over-fiber techniques for 10 Gb/s broadband wireless transmission," in *Wireless World Research Forum*, Ottawa, Canada (WWRF, 2008).
[14] M. Weiß, M. Huchard, A. Stöhr, B. Charbonnier, S. Fedderwitz, and D. Jäger, "60-GHz Photonic Millimeter-Wave Link for Short- to Medium-Range Wireless Transmission Up to 12.5 Gb/s," *IEEE J. Lightw. Technol.,* vol.26, no.15, pp.2424–2429, Aug. 2008.
[15] P. Shen, A. Nkansah, J. James, and N. J. Gomes, "Multilevel Modulated Signal Transmission for Millimeter-Wave Radio over Fiber System" in *Int. Topical Mtg. on Microw. Photon. ,* Gold Coast, Australia, pp. 27-30, Oct. 2008.
[16] J. James, P. Shen, A. Nkansah, X. Liang. and N. J. Gomes, "Full Downlink Transmission of Multilevel QAM Signals over Mm-wave over Fiber System using Phase Modulator and DWDM Filtering," in *4th Asia-Pacific Microwave Photonics Conference (APMP 2009),* Beijing, China, April 2009.
[17] J. Yu, Z. Jia, T. Wang, and G. K. Chang "Centralized Lightwave Radio-Over-Fiber System With Photonic Frequency Quadrupling for High-Frequency Millimeter-Wave Generation," *IEEE Photon. Technol. Lett*., vol. 19, no. 19, pp 1499-1501, Oct. 2007.
[18] IEEE Standard for Local and metropolitan area networks. Part 16: Air Interface for Fixed Broadband Wireless Access Systems, IEEE 802.16^{TM}-2009.
[19] Supplement to IEEE Standard for Information Technology—Telecommunications and Information Exchange Between Systems—Local and Metropolitan Area Networks—Specific Requirements Part 11: Wireless LAN Medium Access Control (MAC) and Physical Layer (PHY) Specifications Amendment 4: Further Higher Data Rate Extension in the 2.4GHz Band, IEEE Standard 802.11g-2003, 2003.
[20] J. Yu, M. Huang, Z. Jia, T. Wang and G. Chang, "A Novel Scheme to Generate Single-Sideband Millimeter-Wave Signals by Using Low-Frequency Local Oscillator Signal," *IEEE Photon. Technol. Lett*., vol. 20, no. 7, pp. 478-480, April. 2008.
[21] C.L. Ying, H.H. Lu, W.S. Tsai, H.C. Peng and C.H. Lee, "To employ SOA-based optical SSB modulation technique in full duplex RoF transport systems," *Progress in Electromagnetics Research Letters*, PIERL 7, vol. 7, pp. 1-13, 2009.
[22] H. Louchet and K. Kuzmin and A. Richter, "Efficient BER Estimation for Electrical QAM Signal in Radio-Over-fiber Transmission," *IEEE Photon. Technol. Lett*., vol. 20, no. 2, pp. 144-146, Jan. 2008.
[23] A. Islam, M. Khan, N. Huda and A. Ali, "Non-Linearity Effects of an OFDM-ROF Link Employing RF Amplifier and EAM," *COIN - ACOFT 2007* - July 2007, Melbourne, Australia.
[24] H. Yang, J. Zeng, Y. Zheng, H. Jung, B. Huiszoon, J. Zantvooort, E. Tangdiongga and A. Koonen, "Evaluation of effects of MZM nonlinearity on QAM and OFDM signals in RoF transmitter," in *Int. Topical Mtg. on Microw. Photon. ,* Gold Coast, Australia, pp. 90-93, Oct. 2008.
[25] J Yu, Z. Jia, T. Wang, and G. Chang, "A Novel Radio-Over-Fiber Configuration Using Optical Phase Modulator to Generate an Optical mm-Wave and Centralized Lightwave for Uplink Connection" *IEEE Photon. Technol. Lett*., vol. 19, no. 3, pp. 140-142, Feb. 2007.
[26] X. Liang, P. Shen, A. Nkansah, J. James, and N. J. Gomes, "Full Downlink Indoor Pico-cellular Network Coverage using a Millimeter-wave over Fiber System," in *Asia Pacific Microwave Conference (APMC2009)*, Singapore, pp. 2344-2347, Dec 2009.
[27] P. Shen, J. James, N.J. Gomes, and P.G. Huggers, "Tuneable Photonic Millimetre Wave Generation using an Optical Phase Modulator and DWDM Thin Film Filters," in *Asia Optical Fiber Communication & Optoelectronic Exposition and Conference*, Shanghai, China, October 2007.
[28] J. James, P. Shen, A. Nkansah and N.J. Gomes, "Optical mm-wave up-conversion of closely separated channels using optical phase modulator," in *6th ISIS workshop*, Stockholm, Sweden, June 2008.
[29] EN 300 744 v1.1.2, "Digital Video Broadcasting; Framing structure, channel coding and modulation for digital terrestrial television", 2008.
[30] H. Ochiai and H. Imai, "On the Distribution of the Peak -to-Average Power Ratio in OFDM Signals," *IEEE Trans. Commun.*, vol. 49, no. 2, pp. 282-289, Feb. 2001.
[31] T.S. Rappaport and S. Sandhu, "Radio-Wave Propagation for Emerging Wireless Personal-Communication Systems, " *IEEE Antenns Propag.* Mag., vol. 36, no.5, pp. 14-23, oct. 1994.
[32] ASH Transceiver Designer's Guide. Dallas, TX: RF Monolithic Inc., 2004, pp.51.

Jeanne James received the B.Eng. degree in communication engineering from Madras University, India, in 2003 and the M.Sc. in broadband and mobile communication networks from the University of Kent, U.K., in 2006, and is currently pursuing the Ph.D. degree in electronic engineering at the University of Kent.

Her research interests include millimeter-wave over fiber systems.

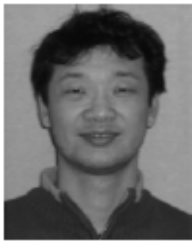

Pengbo Shen received the B.Eng. degree from Shanghai Jiaotong University, Shanghai, China, in 1996, and the PhD degree from University of Kent, Canterbury, UK, both in Electronics Engineering

He has involved with the development of the photonic LO for the Atacama Large Millimeter Wave Array from 1999. His research interests are in the field of microwave photonics and communication, including the generation and distribution of high-quality millimeter-wave signals.

Anthony Nkansah received the B.Eng. (with honors) degree in electronic engineering, the M.Sc. degree in broadband and mobile communication networks and Ph.D degree in electronic engineering from the University of Kent, Canterbury, U.K., in 2000, 2001 and 2007, respectively.

His research interests include low-cost microwave and millimeter-wave radio-over-fiber networks and their deployment within premises.

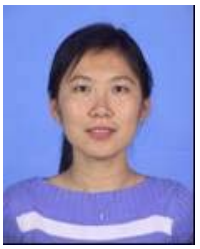

Xing Liang received the M.Sc. degree with distinction in Radio Frequency Communications Engineering, and a Ph.D degree in Mobile and Satellite Communications from the University of Bradford, U.K., in 2002 and 2007, respectively.

Her research interests include millimeter-wave over fiber systems, convergence of networks, digital video broadcasting over satellite, and mobility management in heterogeneous networks.

Nathan J. Gomes (M'92 - SM'06) received the BSc degree from the University of Sussex, UK, in 1984 and the PhD degree from University College London in 1988, both in electronic engineering.

From 1988 to 1989 he held a Royal Society European Exchange Fellowship at ENST, Paris. He has been with the University of Kent since late 1989, where he is now a Reader in Broadband Communications, leading the radio over fiber activities. His present research interests include radio over fiber systems and networks, the photonic generation and transport of millimeter-wave signals, and photoreceivers for such applications.